Ly *et al.*
Progress in Earth and Planetary Science (2023) 10:55
https://doi.org/10.1186/s40645-023-00586-8

Progress in Earth and Planetary Science

RESEARCH ARTICLE

Open Access

Integrated impact assessment of climate change and hydropower operation on streamflow and inundation in the lower Mekong Basin

Steven Ly[1*], Takahiro Sayama[1] and Sophal Try[1,2]

Abstract

Water resources are key to economic development of the Mekong River Basin, but are threatened by climate change and affected by hydropower development. Knowledge of these drivers' integrated impact on future hydrological alterations is limited, especially with respect to flood inundation in the lower basin. This study assesses streamflow and flood extent alterations by reservoir operations and climate change using the latest climate projections. A distributed hydrologic model is used to generate discharge and flood extent. Our findings indicate substantial changes in seasonal and annual peak discharge due to reservoir operations. Under the future hydropower scenario, the discharge at Kratie will change by + 28% (− 10%) during the dry (wet) season. While the effects of hydropower operations vary by season, climate change tends to increase river discharge overall. Under the high-emission scenario, the wet seasonal flow at Kratie will increase by + 7% in the near-future (2026–2050), but change by -5% under integrated impact of climate change and reservoir operations. In the far-future, the wet seasonal flow at Kratie under climate change only (integrated impact) will increase by + 33% (+ 19%). Although climate change is the dominant driver of flow alterations, hydropower development is critical for reducing discharge and flood magnitude. Nonparametric statistical testing shows significant changes in the inundated area by up to + 37% during the projected periods.

Keywords Hydropower, Lower Mekong Basin, River discharge, RRI model

1 Introduction

The Mekong River Basin (MRB), which originates from the Tibetan Plateau, is the largest transboundary river in Southeast Asia. With a length of approximately 4,800 km, the Mekong River travels from its source in China and flows through Myanmar, Laos, Thailand, and Cambodia, before finally reaching its delta and discharging into the South China Sea in Vietnam (MRC 2005). Commonly known as the most fertile ecosystem, more than 70 million inhabitants rely on this river system through fishery and agriculture (Varis et al. 2012). The water resources of the MRB not only provide food and water to its dependents but also contribute significantly to the region's economic development. During the wet monsoon season, the unique flow reversal from the Mekong River to the Tonle Sap floodplain creates the most productive ecosystem, delivering fish and other biodiversity, sediments, and nutrients to Tonle Sap Lake (Arias et al. 2012). In addition, substantial economic development for member countries comes from hydropower development, as explained in the Strategic Plan and Basin Development

*Correspondence:
Steven Ly
steven.ly70@gmail.com
[1] Disaster Prevention Research Institute, Kyoto University, Gokasho, Uji, Kyoto 611-0011, Japan
[2] Faculty of Hydrology and Water Resources Engineering, Institute of Technology of Cambodia, Russian Conf. Blvd., Phnom Penh 120404, Cambodia

of the Mekong River Commission (MRC) (2019a). The potential benefits generated from the hydropower sector alone are almost equivalent to the three major sectors of fisheries, agriculture, and navigation. In addition to electricity supply, hydropower developments could potentially expand agricultural activities during the dry season, function as flood protection during the high-flow season, attract foreign investment, and improve navigation systems (MRC 2019b).

Nonetheless, climate change, along with massive developments in hydropower at a rapid rate, has drastically changed the flow regime of the MRB. According to various studies, climate change is expected to alter temperature and rainfall patterns throughout the region, jeopardizing the hydrology of the basin. Using multiple general circulation models (GCM) from the Coupled Model Intercomparison Project Phase 5 (CMIP5) climate projections, Hoang et al. (2016) analyzed the Mekong River flow under a changing climate. Seasonal and annual river discharge was found to increase (between + 5% and + 16%), but the degree of changes depended on location. In addition, they suggested that the selection of GCM, as well as different versions of climate experiments, influenced the results of the flow changes. Try et al. (2020b) used high-resolution atmospheric general circulation model (AGCM) outputs to estimate the river flow alterations and hydrological extremes in the MRB due to changing climate. Their study estimated a + 14% increase in annual precipitation and high flow (Q5) increased up to + 30% at Kratie in the downstream of MRB under the high-emission scenario of representative concentration pathway (RCP8.5). Moreover, under the 4 K increasing scenario from the database for Policy Decision-Making for Future Climate Change (d4PDF), Try et al. (2020a) found that increasing precipitation contributed to the intensity of future flood events, resulting in an increase in the flooding area and volume by nearly + 40%. In addition to climate change, the MRB's water resources have been strained by the hydropower construction. Despite its benefits, such rapid developments are expected to impact water resource management and the seasonality of the flow regime. Many hydropower projects are being constructed and proposed throughout the basin, including 11 hydropower projects along the Lower Mekong Basin (LMB). Most will be completed in the next 10–20 years (Hecht et al. 2019). Several studies (Piman et al. 2013a; Liu et al. 2016; Räsänen et al. 2017; Li et al. 2017; Do et al. 2020) have studied the effects of hydropower construction in the MRB from various perspectives. The degree of impact differs from one study to another based on the study periods, dam scenarios, and reservoir operation rules. However, they shared the same conclusion that reservoir operations alter river flow by increasing dry seasonal flow and decreasing wet seasonal flow. Moreover, hydropower can reduce peak flow and delay timing by up to one month (Pokhrel et al. 2018; Shin et al. 2020).

Traditionally, hydropower development and climate change have been analyzed separately; however, acknowledging their interdependence is crucial for effective decision-making and sustainable water resource development (Wang et al. 2017; Hoang et al. 2019; Yun et al. 2020). Unfortunately, the fundamental aspect of the integrated impact stemming from these drivers is often overlooked and inadequately studied, especially the impacts on flood inundation. Some studies prefer to focus on limited impacts of hydropower in only certain regions for case studies, such as the effects of hydropower construction in the Sesan, Sre Pok, and Sekong (3S) river basins (Wild and Loucks 2014; Arias et al. 2014; Piman et al. 2016) and the effect of climate change and reservoir operations in the Upper Mekong Basin (UMB) (Räsänen et al. 2017; Han et al. 2019; Zhong et al. 2021). Motivated by this knowledge gap, this study aims to investigate the combined effects of changing climate and hydropower operations (both existing and future hydropower projects) on flow alterations and flood inundation in the MRB using the Coupled Model Intercomparison Project Phase 6 (CMIP6) projections. This integrated impact assessment not only enhances our comprehension of hydrological changes but also provides valuable insights into the intricate interaction between climate change and reservoir operation in the MRB. This study adopted a distributed rainfall–runoff–inundation (RRI) model coupled with a simple storage model (for reservoir operations) to simulate streamflow and inundation simultaneously for present and future climates.

2 Materials and methods

2.1 Study area

The MRB covers a catchment area of 795,000 km^2 with an annual mean discharge of 14,500 m^3/s (Fig. 1). The climate is governed by the Asian Southwest monsoon, which brings two distinct wet and dry seasons (MRC 2005). The MRB basin consists of two major parts: the UMB in China (so-called Lancang Jiang) and LMB. The MRB has unique and complex hydrological, climatic, and physiographic features. Flood inundation is one of the most important characteristics of the basin because it creates remarkable biodiversity, particularly in the Tonle Sap floodplain and the Mekong Delta (Lamberts 2006; Arias et al. 2012; Hoang et al. 2019; Try et al. 2020b). Its extensive wetlands and floodplains provide the most inland fisheries of 2.6 million tons annually, and other animals are valued at up to 7 million USD (Hortle 2007).

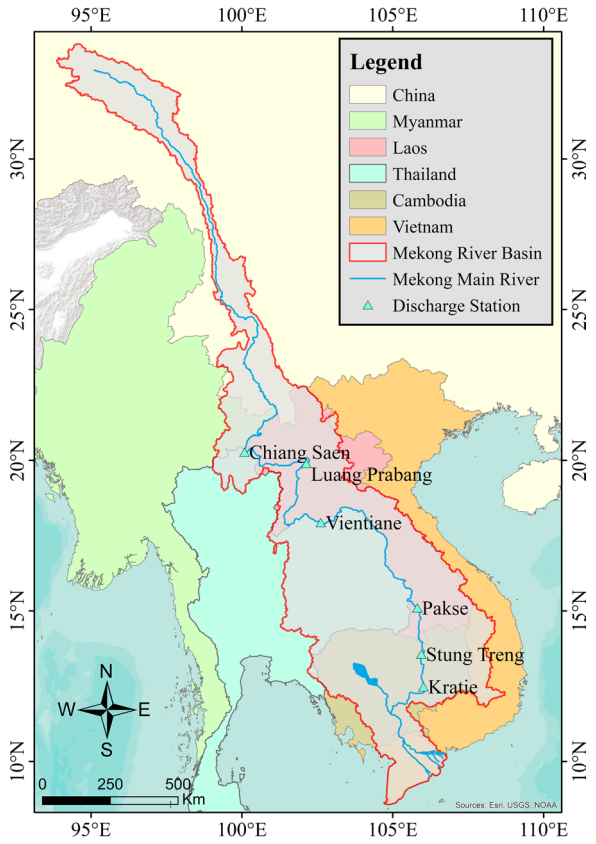

Fig. 1 Location of the Mekong River Basin

2.2 RRI model simulation

The study used the hydrologic RRI model to generate discharge and flood inundation. The two-dimensional distributed RRI model can simultaneously simulate runoff and flood inundation (Sayama et al. 2012, 2015). The model deals with slopes and river channels separately. The hydrological process in the slope was determined by a two-dimensional diffusive wave model, while a one-dimensional model was adopted in the channel flow. The flow interaction between the two is estimated based on different overflowing formulae, depending on water-level and levee-height conditions. Moreover, the adoption of diffusive wave models enables consideration of water exchange interactions between grid cells in all directions (i.e., backwater effect). The adaptive time step Runge–Kutta algorithm was adopted to solve the two-dimensional equations. To prevent simulation instability, the algorithm continues monitoring estimated errors and adjusting simulation time steps until errors were minimized to an appropriate level. A time step of 600 s was assigned for slope-river interactions, whereas the initial time step for river calculation was 60 s. To conduct the long-term simulation, evapotranspiration was taken into account. The RRI model was calibrated from 2000 to 2003 and validated from 2004 to 2007 for the entire MRB in a previous study by Try et al. (2020c). The Shuffled Complex Evolution (SCE-UA) global optimization algorithm, developed by the University of Arizona, was integrated into the RRI model to calibrate the sensitive parameters (Duan et al. 1994). This calibration process specifically targeted five key parameters: river Manning's coefficient, soil surface porosity, lateral hydraulic conductivity, unsaturated porosity, and coefficient for unsaturated hydraulic conductivity. Utilizing the SCE-UA algorithm, the optimization model iterated 500 times to identify the optimal values for these parameters within their designated range of low and high parameter values. Subsequently, the RRI model adopted these optimized parameters to conduct a series of 500 simulations. Before being applied in the long-term simulation of this study, particularly for climate change studies, the RRI model was re-validated from 1982 to 2012. Table 1 presents the RRI model configuration used in this study.

In this study, the simulations were conducted in two steps. Initially, the model was prepared to perform an entire MRB simulation and to assess river discharge at a 2.5' resolution (≈ 5 km). Subsequently, the discharge simulated by the first model served as the boundary condition for the finer-resolution model, which was configured with a higher resolution of 1.5' (≈ 2.7 km). This finer-resolution model was employed to accurately

Table 1 RRI model configuration used in the study

Parameters			Forest	Agriculture	Floodplain
Manning's roughness on slope cell	n_s	–	0.4	0.15	0.015
Soil surface porosity	φ_a	–	0.6	0.6	0.6
Vertical hydraulic conductivity	K_v	cm/s	–	–	0.06
Suction at the wetting front	S_f	m	–	–	0.273
Lateral hydraulic conductivity	K_a	m/s	0.25	0.25	–
Unsaturated porosity	φ_m	–	0.6	0.6	–
Coefficient of unsaturated hydraulic conductivity	β	–	4.0	4.0	–

simulate flood inundations in the LMB (i.e., Cambodia and Vietnam floodplain). For the climate change modeling, it required approximately 7 days to complete a simulation for the entire MRB and roughly 12 days to complete a flood inundation simulation in the LMB on a computer (CPU: Intel Xeon E5-2694, 2.1 GHz, 2 core/4 threats, RAM: 7 GB) after it was parallelized with OpenMP. The model input data included precipitation, topography, land use, evapotranspiration, and river geometry (Table 2). Precipitation data from the Global Precipitation Climatology Centre (GPCC) were used for simulations (Ziese et al. 2018). It was a reanalysis product based on rain gauge data from 67,200 stations around the world. Topographic data were received from the Multi-Error-Removed-Improved-Terrain digital elevation model (Yamazaki et al. 2017). Land-use data were derived from the Moderate Resolution Imaging Spectroradiometer dataset (Friedl et al. 2010). The evapotranspiration was taken from the Japanese 55-year Reanalysis database (Kobayashi et al. 2015). River geometry, river depth D [m] and river width W [m], was approximately estimated from the following equations (Try et al. 2018):

$$D = 0.0015 \times A^{0.7491} \tag{1}$$

$$W = 0.0520 \times A^{0.7596} \tag{2}$$

The model performance was evaluated by four indicators, namely NSE, PBIAS, R^2, and RSR. NSE quantifies the proportion of residual variance in the simulated data relative to the observed data, indicating how closely the hydrograph fits the actual data (Nash and Sutcliffe 1970). NSE = 1 indicates the perfect simulation result. PBIAS metric provides insight into whether the simulated data tend to be biased toward overestimation or underestimation when compared with the observed data (Gupta et al. 1999). PBIAS = 0% is the perfect prediction, while positive and negative values signify underestimation and overestimation bias, respectively. R^2 quantifies the level of collinearity between the simulation and observation, with perfect collinearity corresponding to a value of 1 (Wright 1921). RSR is the error index that includes the benefits of error index statistics and a scaling/normalization factor, where RSR = 0 denotes perfect model simulation (Singh et al. 2005).

$$\mathrm{NSE} = 1 - \frac{\sum (Q_{\mathrm{sim}} - Q_{\mathrm{obs}})^2}{\sum \left(Q_{\mathrm{obs}} - \overline{Q_{\mathrm{obs}}}\right)^2} \tag{3}$$

$$\mathrm{PBIAS} = \frac{\sum (Q_{\mathrm{obs}} - Q_{\mathrm{sim}}) \times 100}{\sum Q_{\mathrm{obs}}} \tag{4}$$

$$R^2 = \frac{\sum \left(\left(Q_{\mathrm{sim}} - \overline{Q_{\mathrm{sim}}}\right)\left(Q_{\mathrm{obs}} - \overline{Q_{\mathrm{obs}}}\right)\right)^2}{\sum \left(Q_{\mathrm{sim}} - \overline{Q_{\mathrm{sim}}}\right)^2 \sum \left(Q_{\mathrm{obs}} - \overline{Q_{\mathrm{obs}}}\right)^2} \tag{5}$$

$$\mathrm{RSR} = \frac{\sqrt{\sum (Q_{\mathrm{obs}} - Q_{\mathrm{sim}})^2}}{\sqrt{\sum \left(Q_{\mathrm{obs}} - \overline{Q_{\mathrm{obs}}}\right)^2}} \tag{6}$$

where Q_{obs} and Q_{sim} are the flow observation and simulation at time t, and $\overline{Q_{obs}}$ and $\overline{Q_{sim}}$ are the mean of flow observation and simulation, respectively.

Table 2 Summary of data adopted in the study

Parameter	Resolution	Source
Precipitation	1° (≈ 120 km)	Ziese et al. (2018)
Topography	3 arc sec (≈ 90 m)	Yamazaki et al. (2017)
Land use	500 m	Friedl et al. (2010)
Evapotranspiration	0.5625° (≈ 55 km)	Kobayashi et al. (2015)

2.3 Hydropower development scenarios

The hydropower database, obtained from the MRC (MRC 2009a, b) and the Asian Development Bank (ADB 2004), includes existing/proposed hydropower in the LMB and Chinese dams in the UMB. Figure 2 illustrates the geographical distribution and active storage capacity of hydropower within the MRB. The majority of these facilities have a storage capacity of less than 0.5 km^3, with Nuozhadu hydropower having the largest capacity of 12.3 km^3. Taking into account existing, under-construction, and proposed hydropower projects, the basin's total storage capacity reaches 107.7 km^3, equivalent to about 23% of its annual discharge volume. This estimation falls well within the range of early projections, varying from 17 to 23% (Hoanh et al. 2010; Kummu et al. 2010; MRC 2011; Hecht et al. 2019). Additionally, the specific total storage capacity in the upstream area of Chiang Saen, Luang Prabang, Pakse, and Kratie hydrological station corresponds to 6%, 8%, 15%, and 22% of the MRB annual discharge volume, respectively. These ratios could serve as a valuable metric to quantify the potential anthropogenic disturbance on terrestrial water cycle resulting from reservoir construction (Vörösmarty et al. 1997). Two hydropower development scenarios were prepared for hydrological analysis in this study. The present development scenario consisted of 98 hydropower projects in the MRB. The future development scenario included 126 hydropower projects, including 23 mainstream dams. Since detailed operation rules were not available in the database, we estimated the general optimized patterns of the dam reservoir outflow for each dam using a simple storage model

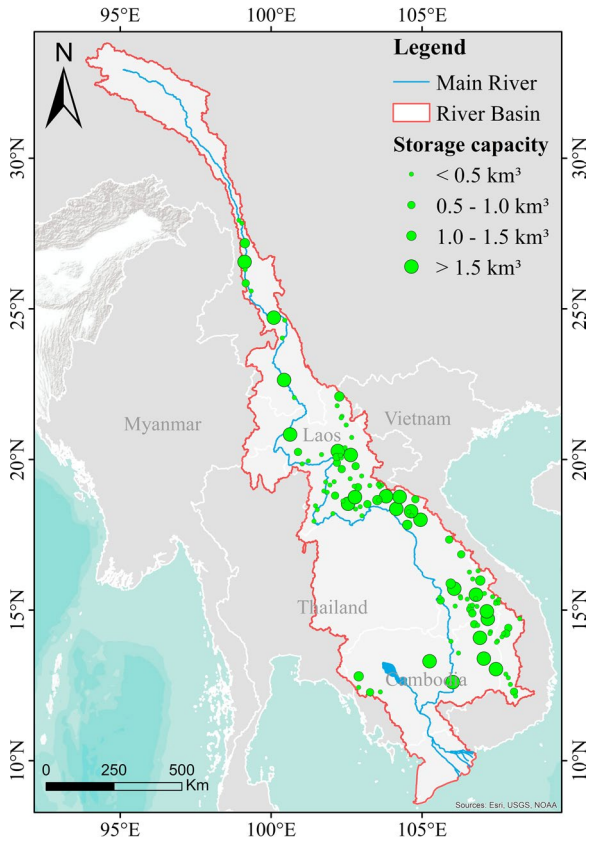

Fig. 2 Location and storage capacity of hydropower in the Mekong River Basin

proposed by Ly et al. (2021). Similar approach has also been adopted in various studies where reservoir operation rule was not available (Räsänen et al. 2012; Lauri et al. 2012; Hoang et al. 2019). The simple storage model estimated the optimum reservoir outflow pattern for each dam using basic information such as river inflow, reservoir storage, and turbine flow capacity. The objective function of the model was to maximize production outflow (i.e., outflow through turbines), thus maximizing hydropower generation considering the local flow regimes. The simple storage model was then integrated into the RRI model to perform hydrological simulations. See Ly et al. (2021) for further details of the simple storage model adopted in this study. General information of the hydropower project, including its name, purpose, and capacity, is provided in Additional file 1: Table S1.

2.4 Climate change scenarios

General circulation models have been widely developed for climate change studies over time. The newly developed GCMs from CMIP6 promised some improvements and less bias than previous models from CMIP5, particularly in the historical simulations (Eyring et al. 2016; Try et al. 2022). The outputs of eight GCMs from CMIP6 were selected for this study (Table 3). Two Share Socioeconomic Pathways (SSP) scenarios were adopted: SSP2-4.5 (middle of the road) and SSP5-8.5 (fossil-fueled development). The present period represented 1980–2014, and the future period (2026–2100) was separated into three 25-year intervals: near-future, mid-future, and far-future. GPCC precipitation was shown to be the most suitable and reliable precipitation product for long-term hydrological modeling in the Mekong region (Try et al. 2020c). Thus, it was chosen as the benchmark rainfall for correcting bias in selected GCMs using the following linear scaling method:

$$P_{\text{daily}}^{\text{BC}} = P_{\text{daily}}^{\text{gcm}} \times \frac{P_{\text{mon}}^{\text{obs}}}{P_{\text{mon}}^{\text{gcm}}} \tag{7}$$

where P_{daily}^{BC} is the daily bias-corrected GCM precipitation, P_{daily}^{gcm} is the daily GCM precipitation, P_{mon}^{obs} is the average monthly GPCC precipitation, and P_{mon}^{gcm} is the average monthly GCM precipitation.

2.5 Statistical Test

2.5.1 Nonparametric Kolmogorov–Smirnov test

For better representations of the variation in flood extent during the study periods, a statistical test

Table 3 List of the GCMs adopted in the study

Model name	Developing research institute	Resolution
ACCESS-CM2	Australian Community Climate and Earth System Simulator Coupled Model version 2.0	1.9°×1.3°
CNRM-CM6-1	Centre National de Recherches Météorologiques Coupled Model Sixth Generation	1.4°×1.4°
GFDL-CM4	Geophysical Fluid Dynamics Laboratory Coupled Model version 4.0	1.3°×1.0°
IPSL-CM6A-LR	Institut Pierre-Simon Laplace Climate Model for Low Resolution	2.5°×1.3°
MIROC6	The Sixth Version of the Model for Interdisciplinary Research on Climate	1.4°×1.4°
MPI-ESM1-2-LR	Max Planck Institute for Meteorology Earth System Model for Low Resolution version 1.2	1.9°×1.9°
MRI-ESM2-0	The Meteorological Research Institute Earth System Model version 2.0	1.1°×1.1°
NorESM2-MM	Norwegian Earth System Model version 2.0 for Medium Resolution of Both Atmosphere–Land and Ocean–Sea Ice	1.3°×0.9°

Kolmogorov–Smirnov (K–S) was used (Massey 1951). The null hypothesis H_0 states that there is no significant difference in the cumulative distribution function between the two sample (i.e., flood extent in the present and future). The test is defined using the following equation:

$$D_{n,m} = \sup_x |F_n(x) - F_m(x)| \tag{8}$$

The null hypothesis H_0 is rejected when the likelihood of the two sample's different distributions exceeds a significance level (α):

$$D_{n,m} > c(\alpha)\sqrt{\frac{n+m}{nm}} \tag{9}$$

where in Eq. (8), empirical distribution functions are denoted by $F_n(x)$ and $F_m(x)$ and supremum function is denoted by **sup**, and in both Eqs. (8) and (9), sample sizes are denoted by n and m. The value of $c(\alpha)$ is 1.36 at a significance level of 5%.

2.5.2 Mann–Kendall Test

The nonparametric, Mann–Kendall, was employed to identify trends in observed discharge used during the validation period. The Mann–Kendall test (Mann 1945; Kendall 1975) has been widely used to detect monotonic trends of variables in hydro-climatic time series such as streamflow, precipitation, and temperature. The Mann–Kendall test statistics is calculated as follows:

$$S = \sum_{i=1}^{n-1}\sum_{j=i+1}^{n} \operatorname{sgn}(x_j - x_i) \tag{10}$$

where n is the number of data points, x_i and x_j are the data values in time series i and $j(j > i)$, respectively, and $\operatorname{sgn}(x_j - x_i)$ is the sign function as:

$$\operatorname{sgn}(x) = \begin{cases} 1 & \text{if } x > 0 \\ 0 & \text{if } x = 0 \\ -1 & \text{if } x < 0 \end{cases} \tag{11}$$

When $n \geq 10$, the standard normal statistics S is approximately normally distributed with the following mean and variance:

$$E(S) = 0 \tag{12}$$

$$\operatorname{var}(S) = \frac{n(n-1)(2n+5) - \sum_{j=1}^{p} t_j(t_j-1)(2t_j+5)}{18} \tag{13}$$

where p is the number of the tied groups in the data set and t_j is the number of data points in the jth-tied group. The standard test statistics Z is computed as follows:

$$Z = \begin{cases} \frac{S-1}{\sqrt{\operatorname{var}(S)}} & \text{if } S > 0 \\ 0 & \text{if } S = 0 \\ \frac{S+1}{\sqrt{\operatorname{var}(S)}} & \text{if } S < 0 \end{cases} \tag{14}$$

The positive value of Z indicates increasing trends, while the negative value represents decreasing trends. The null hypothesis H_0 states that there are no significant trends in the time series. At a significance level (α), H_0 is rejected when $|Z| > Z_{1-\alpha/2}$. According to the standard normal distribution table, the value of $Z_{1-\alpha/2}$ corresponds to 2.576 and 1.96 at a significance level of 1% and 5%, respectively.

2.5.3 Sen's slope estimator

The magnitude of the trend (change per unit time) in the time series was estimated using Sen's slope procedure (Sen 1968). The trend magnitude is calculated as follows:

$$\beta = \operatorname{Median}\left(\frac{x_j - x_i}{j - i}\right), j > i \tag{15}$$

where x_i and x_j are the data values at time j and i, respectively.

2.5.4 Pettitt's test

Pettitt's test (1979) adopted to identify the significant change-point in the annual streamflow time series during the validation period. The nonparametric test statistics can be described as follows:

$$K_T = \max|U_{t,T}| \tag{16}$$

$$U_{t,T} = \sum_{i=1}^{t}\sum_{j=t+1}^{T} \operatorname{sgn}(x_j - x_i) \tag{17}$$

where x_i and x_j are the data values at time j and i, respectively.

The change-point of the time series occurs at K_T, given that the statistics is significant. The null hypothesis H_0 of no change-point is rejected when p is smaller than 0.01 and 0.05 at a significance level of 1% and 5%, respectively. Thus, the associated probability is given as follows:

$$p = 2\exp\left(\frac{-6K_T^2}{T^3 + T^2}\right) \tag{18}$$

3 Results

3.1 Performance of model simulation

Four performance indexes, NSE, PBIAS, R^2, and RSR, were calculated at the four gauging stations along the main river from upstream to downstream: Chiang Saen, Luang Prabang, Pakse, and Kratie during the validation

period. Figure 3 shows the observed and simulated daily discharge during the validation at the selected gauging stations. The observation and simulation of monthly discharge were also compared during the validation period since this study analyzed the flow alterations at monthly and seasonal scales (Fig. 4). Kratie had the highest model performance in both daily (monthly) discharge with NSE = 0.88(0.93), PBIAS = −3.70% (−3.70%), R^2 = 0.88(0.93), and RSR = 0.35(0.27) during the validation (Table 4). The model performance index of monthly discharge at the most upstream station Chiang Saen was NSE = 0.59, PBIAS = −32.9%, R^2 = 0.81, and RSR = 0.64. The four index values of monthly discharge at Luang Prabang were 0.72, −25.2%, 0.82, and 0.53. For the station located in the middle of the LMB at Pakse, the evaluation indicators of monthly discharge were as high as

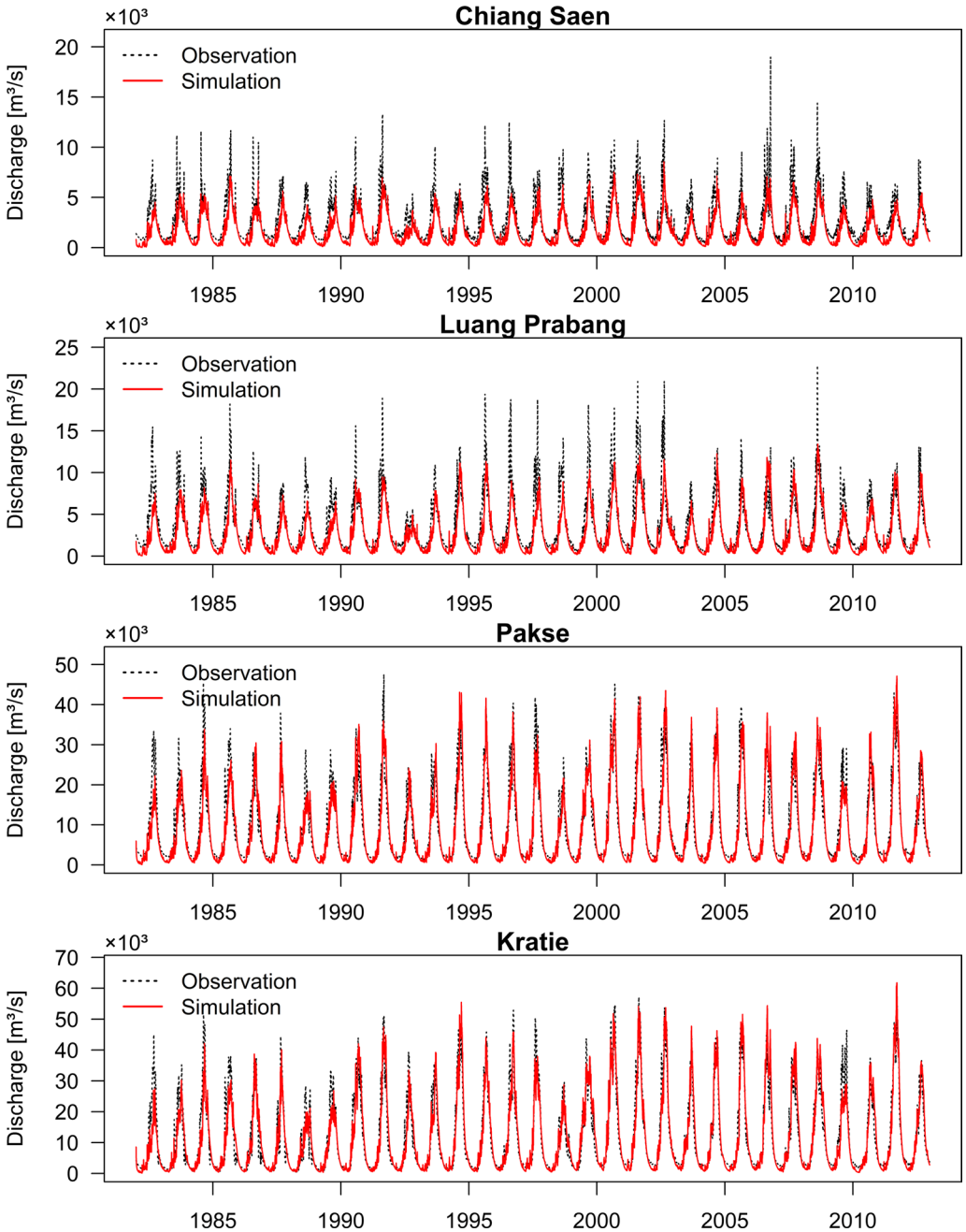

Fig. 3 Observed and simulated daily discharge during the validation period (1982–2012) at Chiang Saen, Luang Prabang, Pakse, and Kratie

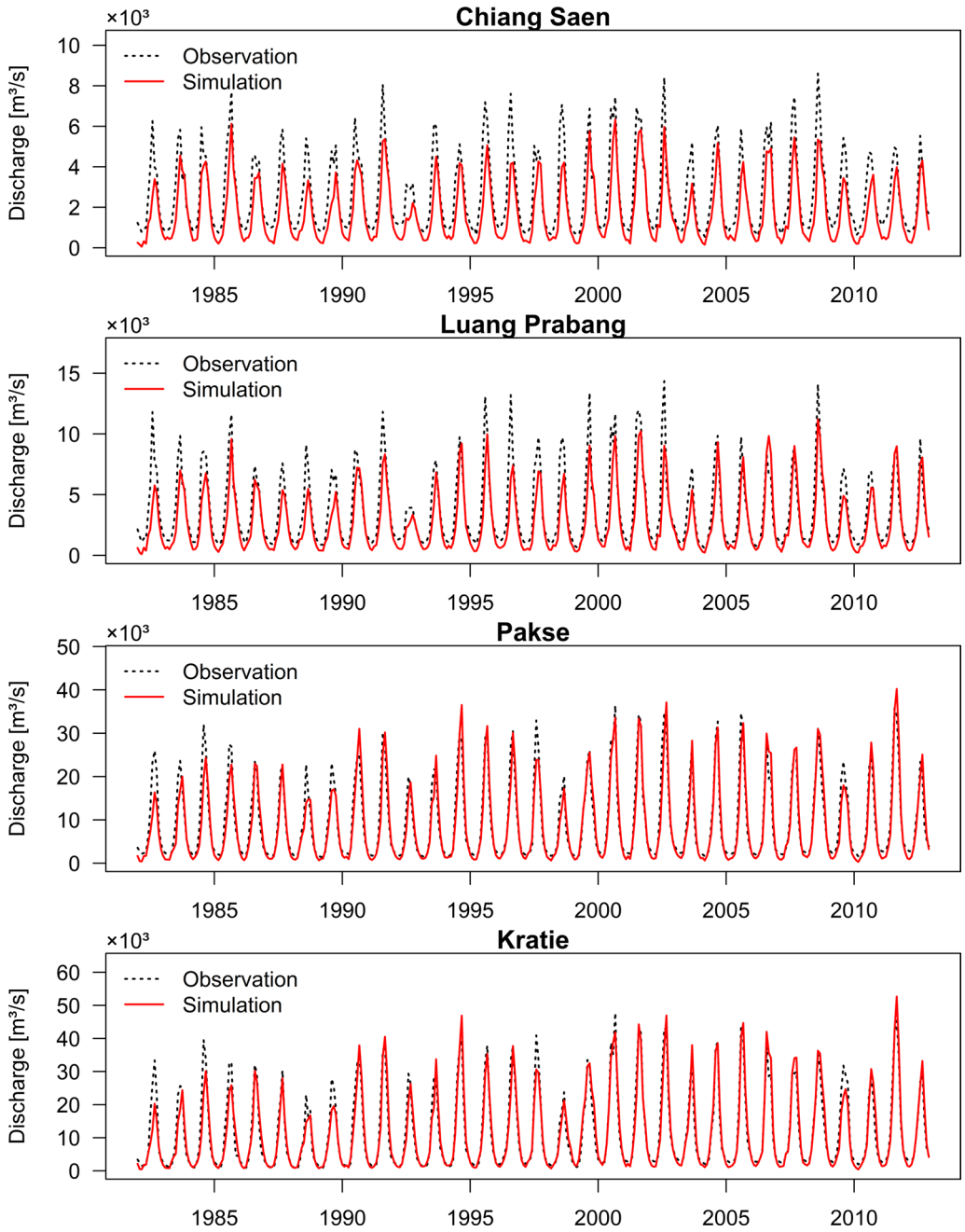

Fig. 4 Observed and simulated monthly discharge during the validation period (1982–2012) at Chiang Saen, Luang Prabang, Pakse, and Kratie

Kratie with NSE = 0.91, PBIAS = −7.50%, R^2 = 0.91, and RSR = 0.30. The underestimations observed in low flow and peak flow at the upstream stations (Chiang Saen and Luang Prabang) can be attributed to various factors. One significant contributing factor was the unaccounted flow regulation caused by the upstream hydropower, as discussed by Hoang et al. (2016) and Räsänen et al. (2012). Multiple studies (Lauri et al. 2012; Sridhar et al. 2019; Try et al. 2022), utilizing different hydrological models such as SWAT and VMod, have also reported similar underestimations for these upstream stations, further supporting aforementioned explanation. Another factor was the lower accuracy of the GPCC precipitation data, owing to the orographic effects and a relatively sparse distribution of rain gauge in this region. Moreover, the exclusion of groundwater dynamics in our simulations may have

Table 4 Model performance of river discharge during the validation period (1982–2012)

Station	NSE	PBIAS (%)	R^2	RSR
Chiang Saen				
Daily	0.52	−32.90	0.70	0.69
Monthly	0.59	−32.90	0.81	0.64
Luang Prabang				
Daily	0.65	−25.30	0.74	0.59
Monthly	0.72	−25.20	0.82	0.53
Pakse				
Daily	0.86	−7.50	0.87	0.38
Monthly	0.91	−7.50	0.91	0.30
Kratie				
Daily	0.88	−3.70	0.88	0.35
Monthly	0.93	−3.70	0.93	0.27

played a contributory role in these underestimations. Despite some underestimations at the upstream station, the results generally indicated favorable agreement between the simulated and observed discharge, particularly in the downstream region. Thus, flood simulations in the LMB under climate change and hydropower operations were further assessed by the RRI model. For the upper Mekong area, we mostly looked at flow alterations at monthly and seasonal scales, as the model performance in simulating monthly discharge was better.

3.2 Performance of bias correction

To order to enhance the performance of precipitation projections, the bias correction of CMIP6 precipitation was carried out using the linear scaling method. This approach aimed to improve the accuracy and reliability of the projected precipitation and its subsequent impact on discharge simulations in the study area. The monthly pattern of GPCC precipitation served as a reference for bias correcting the selected GCMs. The objective of this method was to align the seasonality of selected GCMs with that of GPCC data while preserving the long-term trend of the original GCMs. Figure 5 illustrates the performance of simulated daily discharge before and after bias correction. Prior to bias correction, substantial variation was observed among different GCMs in their simulated discharge. However, following bias correction, these variations were significantly reduced, resulting in a closer alignment with the simulated discharge derived from GPCC data.

3.3 Impacts of hydropower on river discharge

The impacts of hydropower were assessed by the RRI model using GPCC precipitation from 1982 to 2016 with two hydropower development scenarios. Two hydrological stations along the MRB mainstream, Chiang Saen and Kratie, were selected to analyze the flow changes. Due to its location at the UMB outlet, the streamflow analysis at Chiang Saen reflected the direct effect of hydropower operations and hydrological changes in the upper MRB. On the other hand, the analysis of streamflow at Kratie provided insight into the general hydrological patterns of the MRB, as well as flood alteration in the LMB, with a particular focus on the Cambodian floodplain and the Tonle Sap Lake, given that this station monitored all hydropower development activities in the MRB. The analysis at both stations provided useful information on the overall water resources and flood conditions in the MRB, which was beneficial for policymakers and hydropower operators. Figure 6 shows the relative changes in monthly average discharge at Chiang Saen and Kratie over the last three decades under present and future hydropower

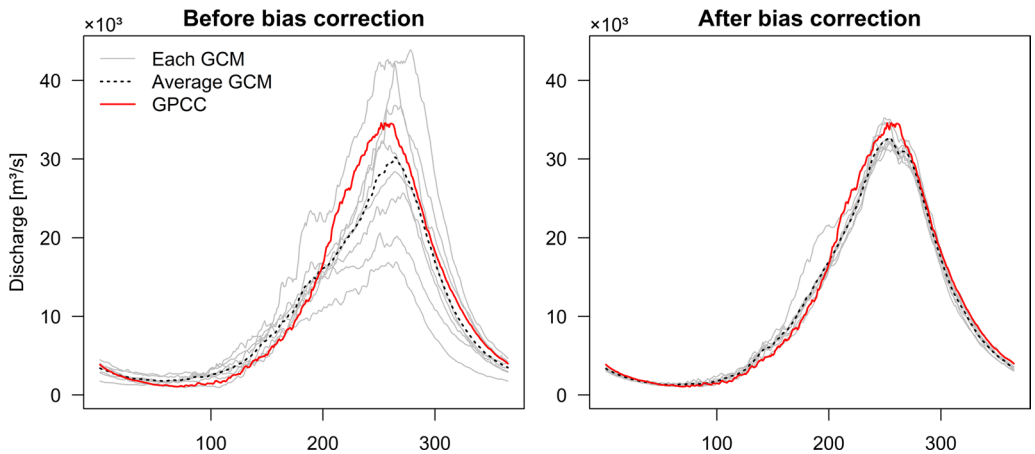

Fig. 5 Daily discharge at Kratie before and after bias correction of CMIP6 GCMs

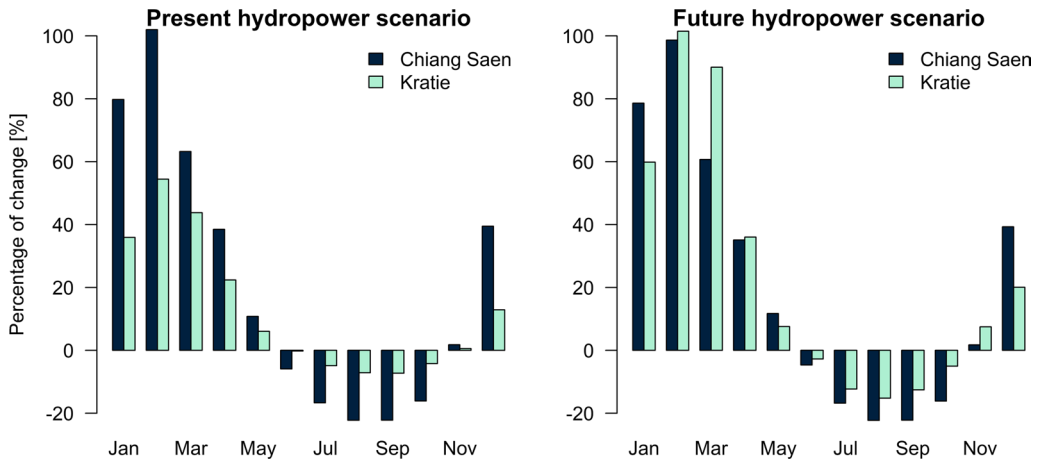

Fig. 6 Relative changes of monthly discharge under different hydropower scenarios

scenarios. Under the present hydropower scenarios (98 dams), the relative changes in monthly discharge at Chiang Saen and Kratie ranged from −22 to + 102% and −7% to + 55%, respectively. The newly proposed dams in the future hydropower scenario further altered the monthly average discharge at both stations. Under the future hydropower scenario, significant changes were observed at Kratie rather than at Chiang Saen, for instance, relative changes in February discharge doubled from the present scenario. A similar tendency was also observed in the wet months, including August and September. Figure 7 presents the relative changes in the average discharge during the dry season (November–April), wet season (May–October), and annual peak. At Kratie, dry seasonal flow increased by + 14% while wet seasonal flow decreased by -5% under the present hydropower scenario, but it doubled to + 28% and −10% in the future scenario, respectively. At Chiang Saen, dry seasonal flow increased by + 36% and wet seasonal flow decreased by -17% under both hydropower scenarios (i.e., there was no significant difference in discharge changes between the hydropower scenarios at Chiang Saen). In addition, future hydropower reduced annual average peak discharge by −29% at Chiang Saen and −13% at Kratie.

3.4 Impacts of climate change on river discharge

To assess the effects of climate change on flow alterations, eight GCMs from CMIP6 projections were utilized as listed in Table 3. The model adopted SSP2-4.5 and SSP5-8.5 scenarios to simulate river discharge for the present climate (1980–2014) and future climate (2026–2100). Figure 8 presents the simulated seasonal discharge under climate change scenarios at Chiang Saen and Kratie. For a better representation of temporal changes in discharge, the future period was divided into three timeframes near-future (2026–2050), mid-future

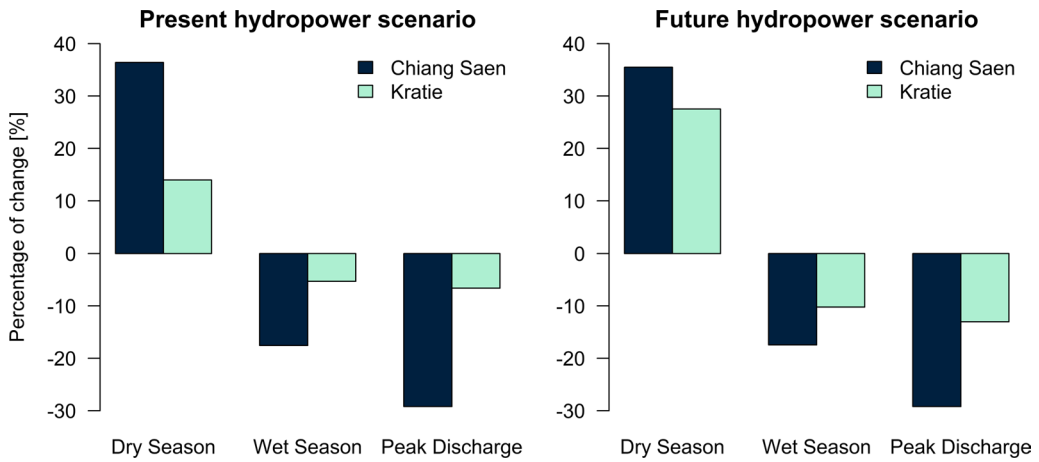

Fig. 7 Relative changes of flow characteristics (seasonal flow and peak discharge) under different hydropower scenarios

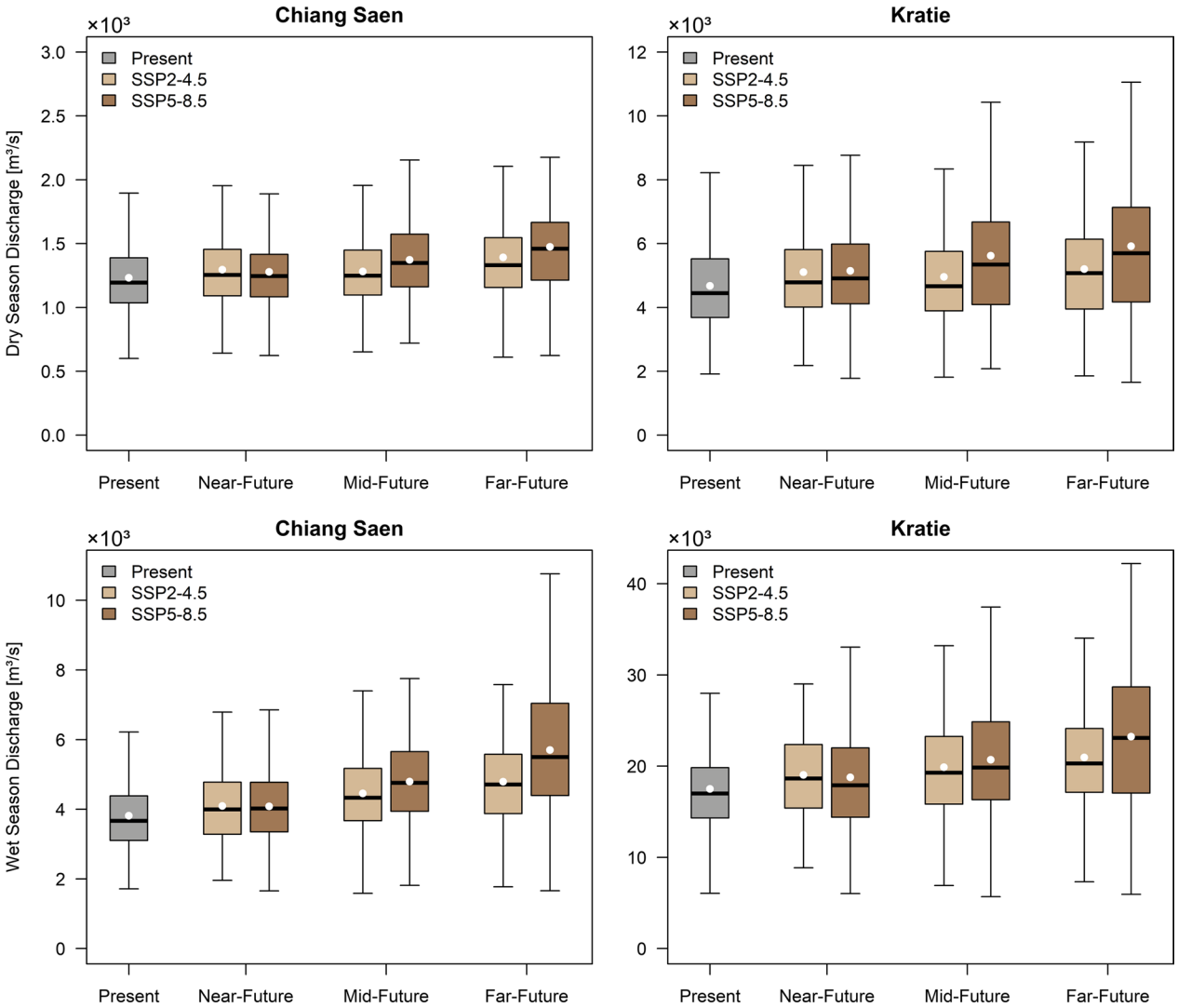

Fig. 8 Simulated discharge in the dry season (top) and wet season (bottom) under present climate and projected future climate scenarios

(2051–2075), and far-future (2076–2100). The results showed a substantial increase at both upstream (Chiang Saen) and downstream (Kratie). Despite the general increasing trend, the SSP5-8.5 scenario had more variation between GCMs, especially in the far-future. The changes in seasonal discharge became more significant in the far-future at all stations during both the dry and wet seasons. Under the SSP5-8.5, the dry season discharge at Chiang Saen and Kratie increased from + 4% and + 10% in the near-future to + 20% and + 27% in the far-future, respectively. Discharge changes were slightly greater during the wet season than those in the dry season. It increased from + 7% (+ 7%) in the near-future to + 50% (+ 33%) in the far-future at Chiang Saen (Kratie). Overall, the degree of climate change impacts increased with the future timeframe (i.e., near-future period < mid-future period < far-future period). On the other hand, peak discharge was computed and analyzed on the annual timescale for both present and future conditions. The time series of the simulated annual peak discharge under climate change scenarios (SSP2-4.5 and SSP5-8.5) from 1980 to 2100 is presented in Fig. 9. There was a noticeable increase in peak discharge in the far-future, especially under the SSP5-8.5 scenario. In comparison with the present condition, the peak discharge in the far-future at Chiang Saen and Kratie increased by an average of + 50% and + 43%, respectively. These increases in peak discharge would lead to a surge in flooded area in the LMB.

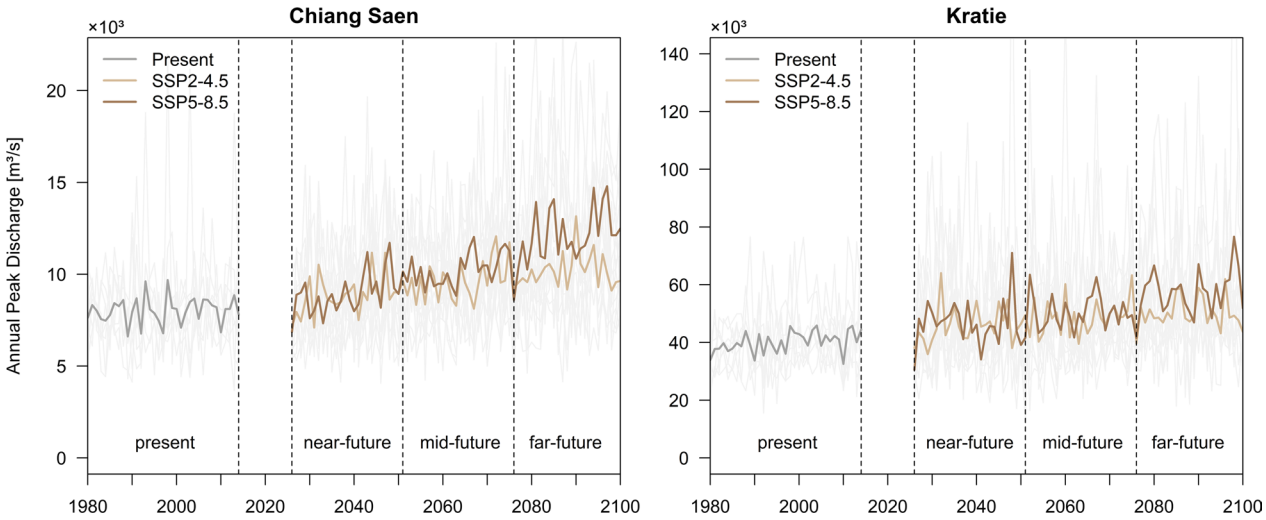

Fig. 9 Time series of simulated annual peak discharge from 1980 to 2100 under present climate and projected future climate scenarios

3.5 Integrated impact of hydropower and climate change on river discharge

The integrated impact of hydropower and climate change on flow alterations were evaluated on a seasonal timescale using the RRI model. Future changes were analyzed in three different timeframes: near-future, mid-future, and far-future. Overall, the seasonal discharge showed noticeable changes at all stations, but the direction and degree of changes differed between the seasons. At Chiang Saen, no significant changes in discharge were detected between the two hydropower development scenarios due to the fact that there was no newly proposed dam in the upper part of this station. Figure 10 shows the simulated seasonal discharge under reservoir operations and climate change (SSP5-8.5) at Chiang Saen and Kratie. Discharge increased gradually from time to time during the dry season. The impacts can be seen clearly at both stations, where reservoir operations (especially the future dam scenario) further increased the discharge in addition to climate change. Under future hydropower and climate change (SSP5-8.5 scenario), the relative changes in average dry seasonal flow at Chiang Saen and Kratie in the far-future increased by up to + 60% and + 61%, respectively. On the contrary, during the wet season, climate change substantially increased the discharge, while reservoir operations tended to reduce the effect of climate change by decreasing the discharge. Nevertheless, reservoir operations have not been able to fully diminish the effects of climate change. Consequently, it was still noticeable at both stations. Under climate change only (SSP5-8.5 scenario), the relative changes in average wet seasonal flow at Chiang Saen and Kratie in the far-future increased by up to + 49% and + 33%, respectively. However, future hydropower could reduce the total changes to + 32% and + 19%, respectively. Although the effects of climate change dominated reservoir operations in most scenarios, there were exceptional cases in the near-future. Under climate change only (SSP5-8.5), the average wet seasonal flow at Chiang Saen and Kratie increased by up to + 7% (both stations) nonetheless, it was reduced to −13% and −5%, respectively, under combined impacts (Table 5). In the annual peak discharge, some compromise occurred between reservoir operations and climate change to some degree. A time series of annual peak discharge under combined impacts at Chiang Saen and Kratie is presented in Fig. 11. Depending on the scenarios, time frame, and location, the findings indicated that hydropower construction could mitigate climate change effects, as summarized in Table 5.

3.6 Integrated impact of hydropower and climate change on flood extent

Flooding is one of the most important characteristics of the MRB because its floodplain creates remarkable biodiversity in the LMB. To further understand the effects of reservoir operations and climate change projections on the flood extent in the LMB, simulations were performed at a finer resolution of 1.5' (≈ 2.7 km). A water depth of 0.5 m was selected to distinguish between flooded and non-flooded area. Moreover, the K-S test was conducted to determine the significant difference in flood variation during the study periods. The results indicated an increase in flood extent in all scenarios, ranging from + 2 to + 37%, compared with the present condition (Table 6). Figure 12 shows the changes in flood extent in the present and future

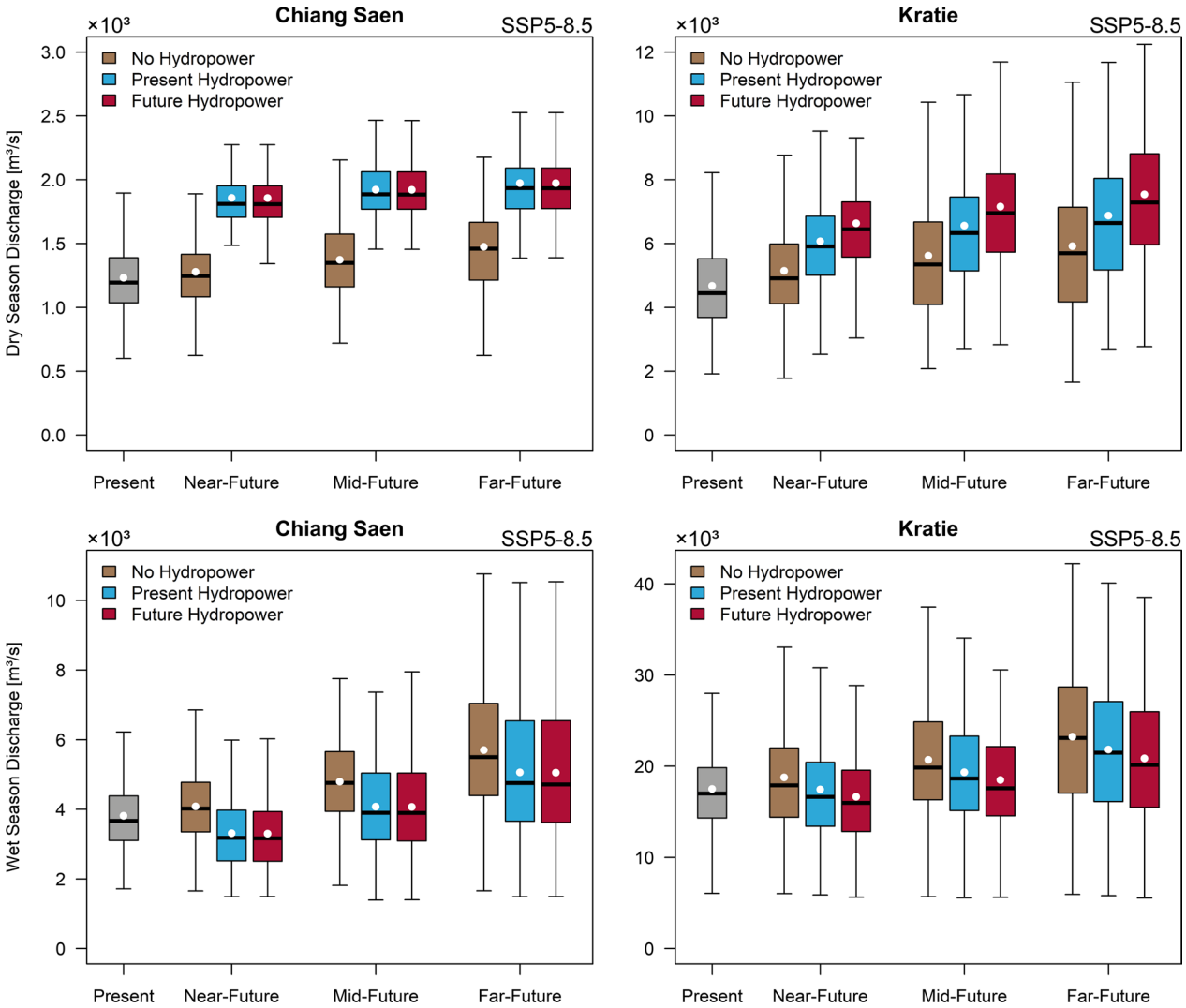

Fig. 10 Simulated discharge in the dry season (top) and wet season (bottom) under reservoir operations and climate change (SSP5-8.5)

conditions under hydropower development scenarios and climate change projections (SSP5-8.5). The largest relative changes occurred under the climate change-only scenario in the far-future, up to + 37%. The smallest relative changes were observed under the combined impacts in the near-future, at + 2%. The K-S test results showed significant differences for most scenarios at a 95% confidence level ($p < 0.05$), except for scenarios in the near-future, which showed no significant difference ($p > 0.05$) between present and future conditions. Our findings indicated that hydropower played a significant role in reducing flood inundation in the LMB, although the climate change effects remained to some degree.

4 Discussion

This study investigated the seasonal flow and flood extent changes caused by future climate change and reservoir operations in the MRB using the RRI model with CMIP6 GCMs. Various bias-corrected GCMs with different emission scenarios were considered to provide more robust and less uncertain results.

4.1 Main findings

Our results suggested that reservoir operations substantially changed the seasonal flow in the MRB, particularly under future hydropower development scenarios. The simulation results of the reservoir operations indicated that the dry season flow would increase and the wet

Table 5 **a** Summary of relative changes of dry season discharge in the future under different scenarios **b** Summary of relative changes of wet season discharge in the future under different scenarios **c** Summary of relative changes of annual peak discharge in the future under different scenarios

a

Dry season	Chiang Saen			Kratie		
	Dam (%)	CC (%)	Combined (%)	Dam (%)	CC (%)	Combined (%)
Near-future						
SSP2-4.5	+44	+5	+52	+30	+9	+41
SSP5-8.5	+45	+4	+51	+29	+10	+42
Mid-future						
SSP2-4.5	+44	+4	+50	+31	+6	+39
SSP5-8.5	+40	+11	+56	+27	+20	+53
Far-future						
SSP2-4.5	+39	+13	+56	+31	+11	+45
SSP5-8.5	+34	+20	+60	+27	+27	+61

b

Wet season	Chiang Saen			Kratie		
	Dam (%)	CC (%)	Combined (%)	Dam (%)	CC (%)	Combined (%)
Near-future						
SSP2-4.5	−19	+7	−13	−11	+9	−4
SSP5-8.5	−19	+7	−13	−11	+7	−5
Mid-future						
SSP2-4.5	−17	+17	−3	−11	+14	+1
SSP5-8.5	−15	+26	+7	−11	+18	+6
Far-future						
SSP2-4.5	−15	+26	+6	−11	+20	+6
SSP5-8.5	−11	+49	+32	−10	+33	+19

c

Peak discharge	Chiang Saen			Kratie		
	Dam (%)	CC (%)	Combined (%)	Dam (%)	CC (%)	Combined (%)
Near-future						
SSP2-4.5	−11	+10	−2	−11	+14	+1
SSP5-8.5	−12	+11	−2	−11	+16	+3
Mid-future						
SSP2-4.5	−8	+20	+10	−11	+21	+8
SSP5-8.5	−7	+28	+18	−11	+23	+12
Far-future						
SSP2-4.5	−6	+27	+19	−11	+25	+11
SSP5-8.5	−4	+50	+44	−10	+43	+29

The future hydropower development scenario was adopted in the calculation

season flow would decrease at the two investigated stations. Flow alterations were detected from the upstream (Chiang Saen) to the downstream (Kratie). Results from the monotonic trend analysis and change-point detection are shown in Table 7. No significant trends were detected at a 99% confidence level ($|Z| < 2.576$). Nonetheless, a significant trend with a 95% confidence level ($|Z| > 1.96$) was identified at a downstream station Kratie. Pettitt's

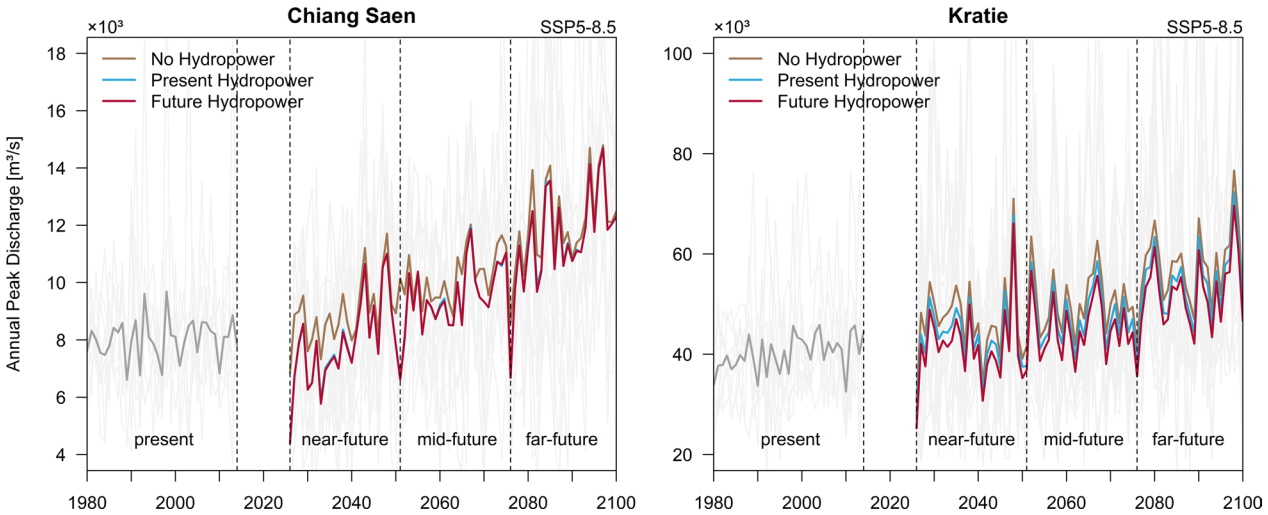

Fig. 11 Time series of simulated annual peak discharge from 1980 to 2100 under reservoir operations and climate change (SSP5-8.5)

Table 6 Changes in flood inundation area and the K–S test results under climate change and integrated impact

Scenarios	Present	Near-future	Mid-future	Far-future
Climate change	23,299 km^2	26,341 km^2 (+13%)*	28,291 km^2 (+21%)*	31,853 km^2 (+37%)*
Climate Change + Existing dam		24,720 km^2 (+6%)	26,813 km^2 (+15%)*	30,568 km^2 (+31%)*
climate change + future dam		23,762 km^2 (+2%)	25,887 km^2 (+11%)*	29,649 km^2 (+27%)*

*Statistically significant at the 5% significance level

test indicated that most of the series were homogeneous, showing no significant changes. Except for Kratie, a significant shift with a 95% confidence level ($p = 0.019$) was detected in 1993. It was confirmed by several studies that hydropower operations were the primary factor responsible for flow alterations during that period rather than climate change (Cochrane et al. 2014; Dang et al. 2016; Binh et al. 2020). Under reservoir operations, the dry seasonal flow alterations started as early as December (early dry season), while the largest relative changes occurred in February. These changes could reduce water shortage issues and potentially increase agricultural activities for local residents.

Climate change was estimated to affect flow regimes, as reported in our study and several others (Ngo et al. 2018; Hoang et al. 2019; Han et al. 2019; Try et al. 2020a, b). In addition, water resources were changing on a global scale, including the MRB. It was projected to alter the intensity and pattern of precipitation and evaporation, thus affecting runoff at the local scale (IPCC 2007). Our findings from the eight CMIP6 GCMs suggested that climate change increased seasonal discharge and annual peak in all scenarios throughout the century. Besides, reservoir operations reduced the effect of climate change by decreasing wet seasonal discharge and annual peak discharge across all scenarios and timeframes. The increased dry seasonal flow would provide additional water supply and extensive irrigation benefits to local residents. However, an increase in wet seasonal flow, especially peak discharge, would result in excessive inundated area in the LMB floodplain, affecting both the local residents' livelihood and essential infrastructures. Although there were some compromises between the two main drivers, climate change remained the dominant factor of flow alterations in the MRB.

Our findings indicated that climate change would trigger flood risk in the LMB under all scenarios by increasing the inundated area by up to +37% at the end of the century. However, hydropower development, especially future hydropower dams, could effectively reduce the flood magnitude in the flood-prone area of the LMB. The study further evaluated the significance of flood risk using the statistical K-S test. Except in the near-future timeframe, the changes in the inundated area were shown to be significant in most scenarios.

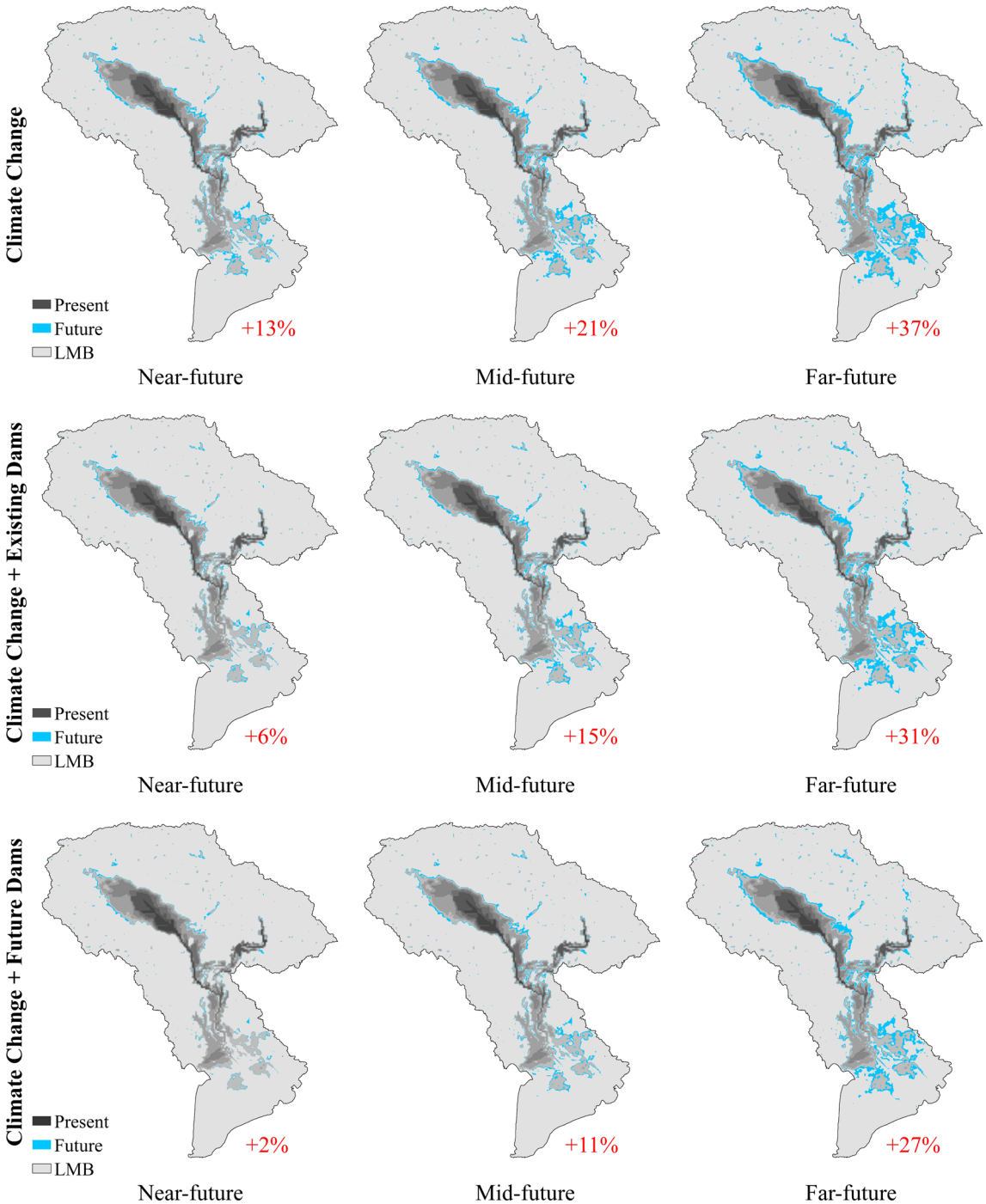

Fig. 12 Comparison of inundated area under different hydropower development and climate change scenarios (SSP5-8.5)

4.2 Comparison to existing research

Various researches evaluated the impacts of hydropower operations on river discharge at Chiang Saen and Kratie using different hydrologic models (Hoanh et al. 2010; Lauri et al. 2012; Piman et al. 2013b). All previous studies suggested considerable changes in seasonal discharge, which are consistent with our findings. Hoanh et al. (2010) used the SWAT and IQQM models to analyze the impact of hydropower development in the MRB from 1985 to 2000. Their study reported a -17% and -8% decrease in the high-flow season and a + 60% and + 28% increase in the low-flow

Table 7 Results of the trend analysis and change-point detection tests of annual discharge over the period 1982–2012

Station	Z_{MK}	Sen's slope	Pettitt test
Chiang Saen	0.034	0.159	NS
Luang Prabang	−0.952	−12.92	NS
Pakse	0.749	36.60	NS
Kratie	2.416*	108.6	*

NS Statistically not significant

*Statistically significant at the 5% significance level

**Statistically significant at the 1% significance level

season at Chiang Saen and Kratie, respectively. Similarly, using the VMod model, Lauri et al. (2012) investigated the effect of hydropower from 1982 to 1992 and showed that wet seasonal flow would decrease by -19% and -10%, while dry seasonal flow would increase by + 55% and + 44% at Chiang Saen and Kratie, respectively. The findings of Piman et al. (2013b), who evaluated the changes in average seasonal flow under future hydropower scenarios from 1986 to 2000 at only Kratie, are also in line with Lauri et al. (2012) and Hoanh et al. (2010). Our findings concur with the directional discharge changes observed by their study, although there are some differences in magnitude due to variations in boundary conditions, hydrologic model selection, operational conditions, and study duration. Compared to other studies, this study has projected a relatively modest rise in the dry season at Chiang Saen. Under the future hydropower, our results suggested a -17% and -10% decrease in wet seasonal flow and a + 36% and + 28% increase in dry seasonal flow at Chiang Saen and Kratie, respectively.

Many studies also assessed the impact of climate change on river hydrology in the MRB using different future climate change projections. The majority of the studies focused on the flow variation at Kratie. Hoang et al. (2016) adopted VMod hydrological model along with the CMIP5 GCMs to study the effect of climate change on flow characteristics during the period of 2036–2065, as compared to the baseline period of 1971–2000. Their results showed that river discharge at Kratie was expected to increase in both dry and wet seasons. Moreover, relative discharge increases were greater during the dry season (up to + 40% in April) although absolute discharge increases were more substantial during the wet season. Using the regional climate data (RCM), Hoanh et al. (2010) studied the impact of climate change (2010–2050) by the SWAT model. Their findings indicated that the discharge at Kratie would increase by + 23% in the dry season and by + 11% in the wet season, compared with the baseline period (1985–2000). Our estimations are consistent with those of other studies, indicating a + 20% increase in the dry seasonal flow and a + 18% increase in the wet seasonal flow at Kratie during the mid-future period (2051–2075). Based on the analysis of five GCMs from CMIP5, Hoang et al. (2016) reported that the projected annual discharge changes at Kratie ranged from + 3% (CCSM4) to + 8% (ACCESS1-0) under the RCP4.5 and -7% (HadGEM2-ES) to + 11% (MPI-ESM-LR) under the RCP8.5. In our study, using a more comprehensive ensemble of eight GCMs from CMIP6, a wider range of changes has been observed, ranging from -4% (NorESM2-MM) to + 35% (GFDL-CM4) under the SSP2-4.5 and from -12% (MPI-ESM1-2-LR) to + 37% (IPSL-CM6A-LR) under the SSP5-8.5. The enhanced capability of CMIP6, particularly its broader equilibrium climate sensitivity, have contributed to these more robust estimations in our analysis. Notably, Try et al. (2022) examined the performance of CMIP5 and CMIP6 projections in the MRB, finding that CMIP6 outputs demonstrated higher correlation and lower error coefficients compared CMIP5 outputs, further validating the improvements in the CMIP6 models.

Using the RRI model with AGCM outputs, Try et al. (2020b) found that climate change (2075–2099) increased the inundated area in the LMB between + 19% and + 43%. Wang et al. (2017) used the GBHM model with CMIP5 GCMs to show significant increases in the mean annual maximum flood and flood frequency in the far-future (2070–2099) over the Mekong region, particularly in the lower basin. Perera et al. (2017) utilized the BTOP model and RRI model with bias-corrected MRI-AGCM to emphasize the future severity of flooding and agricultural damage (2075–2099) in the LMB. These studies agree with our findings regarding the direction and magnitude of changes. Results from our simulation showed that peak discharge at Kratie would increase up to + 43%, and inundated area in the LMB would increase up to + 37% under climate change in the far-future. Apart from climate change, reservoir operations are another aspect to consider when analyzing flood extent in the MRB. Yun et al. (2020) used the VIC model to analyze the impact of both changing climate conditions and the construction of hydropower facilities on flood intensity and frequency. Their study suggested some benefits of hydropower in eliminating flood risk, but their study period for climate change was between 2008 and 2016. In addition to existing studies, this study analyzed the integrated impact of reservoir operations and climate change to the end of the century and highlighted the important role of hydropower in mitigating the effect of climate change. Moreover, our study adopted the latest climate projections dataset from CMIP6, with different SSP scenarios.

4.3 Limitations and uncertainties

This study assessed the effects of changing climate conditions and hydropower operations using a hydrologic model. Several aspects, including groundwater, irrigation water withdrawal, and land-use change, were not considered in the simulations. For both current and future climates, it was assumed that land use would remain constant during the study period. This study did not incorporate the possible alterations in evapotranspiration that may arise in the future. Instead, its average historical values were used as a baseline in simulating the future climate change scenarios. Future studies should include these drivers to provide a broader perspective on the hydrological alterations of the MRB. In addition, a rectangular approximation for river geometry was adopted in the study due to the limited data availability. In general, such an approximation is not ideal for flood inundation analysis. However, the flood inundation in the Mekong River is relatively large that the river is submerged under the inundation. In such a case, the river cross section becomes less important. Therefore, a rectangular approximation was used to estimate the river cross-section, where actual river geometry is unavailable in this study. Nonetheless, actual river geometry would provide a better result on flood prediction. Owing to the limited information on reservoir operation rules, our study used a simple storage model to estimate the general optimized patterns of reservoir operations and assumed that all hydropower was operated to maximize energy production. In actual operations, hydropower may have multiple functions, including drought relief, ecological sustainability, flood control, sediment control, and water supply. Therefore, different reservoir operation scenarios should be considered in future assessments. The simulations of flood inundation were carried out at a resolution of 2.7 km owing to the computational capacity. A finer resolution would provide more accurate predictions. On the other hand, there were two main sources of uncertainties in this study: data input uncertainties induced by different GCMs and model parameters uncertainties. Although this study applied bias correction to the future projected climate data, the application of RCM or downscaled GCM would reduce the model projections' uncertainties and provide better predictions of rainfall patterns. Moreover, the consideration of multi-model would be ideal to reduce the uncertainties of future river discharge predictions.

5 Conclusion

This study assesses changes in river discharge and flood inundation induced by hydropower facilities and future climate variation in the MRB using a hydrologic RRI model coupled with a reservoir model. This study adopts bias-corrected CMIP6 GCMs to analyze the changes in dry seasonal flow, wet seasonal flow, annual peak discharge, and flood extent for the current period (1980–2014) and future period (2026–2100). Our results indicate noticeable changes in seasonal flow and highlight the important role of hydropower in reducing annual peak discharge, thus mitigating the flood risk in the LMB. Climate change has forcefully modified the flow regime from a monthly to an annual scale. The seasonal discharge and annual peak discharge increased considerably in all climate change scenarios. The largest changes are observed in the far-future under the high-emission scenario (SSP5-8.5). During the wet season, discharge at Kratie increased by + 7% in the near-future and by + 33% in the far-future; nonetheless, the flow changes under integrated impact decreased to -5% and + 19%, respectively. Despite the effect of reservoir operations, climate change remains the dominant contributor to hydrological changes in the MRB. However, the magnitude of the impact varies between timeframes (i.e., near-, mid-, and far-future) and hydropower operations. This study provides concrete insights and broader perspectives for understanding the future hydrological alterations in the Mekong region.

Abbreviations

3S	Sesan, Sre Pok, and Sekong river basins
ADB	Asian Development Bank
AGCM	Atmospheric general circulation model
CMIP5	Coupled Model Intercomparison Project Phase 5
CMIP6	Coupled Model Intercomparison Project Phase 6
d4PDF	Database for Policy Decision-Making for Future Climate Change
GCM	General circulation model
GPCC	Global Precipitation Climatology Centre
K–S	Kolmogorov–Smirnov
LMB	Lower Mekong Basin
MRB	Mekong River Basin
MRC	Mekong River Commission
NSE	Nash–Sutcliffe efficiency
PBIAS	Percent bias
R^2	Coefficient of determination
RCP	Representative concentration pathway
RRI	Rainfall–runoff–inundation
RSR	Root-mean-square error–observations standard deviation ratio
SCE-UA	Shuffled Complex Evolution-University of Arizona
SSP	Socioeconomic pathway
UMB	Upper Mekong Basin

Supplementary Information

The online version contains supplementary material available at https://doi.org/10.1186/s40645-023-00586-8.

Additional file 1: Table S1. List of hydropower projects in the Mekong River Basin.

Acknowledgements

The authors would also like to acknowledge the Mekong River Commission for their assistance in providing the observed datasets.

Author contributions
SL proposed the topic, designed the study, and drafted the manuscript. TS revised and supervised the methodology. ST provided technical support for the modeling process. All authors read and approved the final manuscript.

Funding
This work was supported by the Japanese Government (MEXT) for the first author during his doctoral program in Japan.

Availability of data and materials
All data are available in the main text and the supplementary materials. Additional data may be available from the corresponding authors upon reasonable request.

Declarations

Competing interests
The authors declare that they have no competing interest.

Received: 16 April 2023 Accepted: 29 August 2023
Published online: 05 September 2023

References

ADB (2004) Cumulative impact analysis and Nam Theun 2 contributions—final report. NORPLAN and EcoLao
Arias ME, Cochrane TA, Piman T, Kummu M, Caruso BS, Killeen TJ (2012) Quantifying changes in flooding and habitats in the Tonle Sap Lake (Cambodia) caused by water infrastructure development and climate change in the Mekong Basin. J Environ Manage 112:53–66. https://doi.org/10.1016/j.jenvman.2012.07.003
Arias ME, Piman T, Lauri H, Cochrane TA, Kummu M (2014) Dams on Mekong tributaries as significant contributors of hydrological alterations to the Tonle Sap floodplain in Cambodia. Hydrol Earth Syst Sci 18(12):5303–5315. https://doi.org/10.5194/hess-18-5303-2014
Binh DV, Kantoush SA, Saber M, Mai NP, Maskey S, Phong DT, Sumi T (2020) Long-term alterations of flow regimes of the Mekong River and adaptation strategies for the Vietnamese Mekong Delta. J Hydrol Reg Stud 32:100742. https://doi.org/10.1016/j.ejrh.2020.100742
Cochrane TA, Arias ME, Piman T (2014) Historical impact of water infrastructure on water levels of the Mekong River and the Tonle Sap system. Hydrol Earth Syst Sci 18(11):4529–4541. https://doi.org/10.5194/hess-18-4529-2014
Dang TD, Cochrane TA, Arias ME, Van PDT, de Vries TT (2016) Hydrological alterations from water infrastructure development in the Mekong floodplains. Hydrol Process 30(21):3824–3838. https://doi.org/10.1002/HYP.10894
Do P, Tian F, Zhu T, Zohidov B, Ni G, Lu H, Liu H (2020) Exploring synergies in the water-food-energy nexus by using an integrated hydro-economic optimization model for the Lancang-Mekong River Basin. Sci Total Environ 728:137996. https://doi.org/10.1016/j.scitotenv.2020.137996
Duan Q, Sorooshian S, Gupta VK (1994) Optimal use of the SCE-UA global optimization method for calibrating watershed models. J Hydrol 158(3–4):265–284. https://doi.org/10.1016/0022-1694(94)90057-4
Eyring V, Bony S, Meehl GA, Senior CA, Stevens B, Stouffer RJ, Taylor KE (2016) Overview of the Coupled Model Intercomparison Project Phase 6 (CMIP6) experimental design and organization. Geosci Model Dev 9(5):1937–1958. https://doi.org/10.5194/GMD-9-1937-2016
Friedl MA, Sulla-Menashe D, Tan B, Schneider A, Ramankutty N, Sibley A, Huang X (2010) MODIS collection 5 global land cover: algorithm refinements and characterization of new datasets. Remote Sens Environ 114(1):168–182. https://doi.org/10.1016/J.RSE.2009.08.016
Gupta HV, Sorooshian S, Yapo PO (1999) Status of automatic calibration for hydrologic models: comparison with multilevel expert calibration. J Hydrol Eng 4(2):135–143. https://doi.org/10.1061/(ASCE)1084-0699(1999)4:2(135)
Han Z, Long D, Fang Y, Hou A, Hong Y (2019) Impacts of climate change and human activities on the flow regime of the dammed Lancang River in Southwest China. J Hydrol 570:96–105. https://doi.org/10.1016/J.JHYDROL.2018.12.048
Hecht JS, Lacombe G, Arias ME, Dang TD, Piman T (2019) Hydropower dams of the Mekong River Basin: a review of their hydrological impacts. J Hydrol 568:285–300. https://doi.org/10.1016/j.jhydrol.2018.10.045
Hoang LP, Lauri H, Kummu M, Koponen J, van Vliet MTH, Supit I, Leemans R, Kabat P, Ludwig F (2016) Mekong River flow and hydrological extremes under climate change. Hydrol Earth Syst Sci 20(7):3027–3041. https://doi.org/10.5194/hess-20-3027-2016
Hoang LP, van Vliet MTH, Kummu M, Lauri H, Koponen J, Supit I, Leemans R, Kabat P, Ludwig F (2019) The Mekong's future flows under multiple drivers: how climate change, hydropower developments and irrigation expansions drive hydrological changes. Sci Total Environ 649:601–609. https://doi.org/10.1016/j.scitotenv.2018.08.160
Hoanh CT, Jirayoot K, Lacombe G, Srinetr V (2010) Impacts of climate change and development on Mekong flow regimes first assessment—2009. MRC technical paper no. 29. Mekong River Commission, Vientiane
Hortle KG (2007) Consumption and the yield of fish and other aquatic animals from the Lower Mekong Basin. MRC technical paper no. 16. Mekong River Commission, Vientiane
IPCC (2007) The physical science basis. Contribution of working group I to the fourth assessment report of the Intergovernmental Panel on Climate Change. Cambridge University Press, Cambridge and New York
Kendall MG (1975) Rank correlation methods, 4th edn. Charles Griffin, London
Kobayashi S, Ota Y, Harada Y, Ebita A, Moriya M, Onoda H, Onogi K, Kamahori H, Kobayashi C, Endo H, Miyaoka K, Takahashi K (2015) The JRA-55 reanalysis: general specifications and basic characteristics. J Meteorol Soc Japan Ser II 93(1):5–48. https://doi.org/10.2151/JMSJ.2015-001
Kummu M, Lu XX, Wang JJ, Varis O (2010) Basin-wide sediment trapping efficiency of emerging reservoirs along the Mekong. Geomorphology 119(3–4):181–197. https://doi.org/10.1016/j.geomorph.2010.03.018
Lamberts D (2006) The Tonle Sap Lake as a productive ecosystem. Int J Water Resour Dev 22(3):481–495. https://doi.org/10.1080/07900620500482592
Lauri H, de Moel H, Ward PJ, Räsänen TA, Keskinen M, Kummu M (2012) Future changes in Mekong River hydrology: impact of climate change and reservoir operation on discharge. Hydrol Earth Syst Sci 16(12):4603–4619. https://doi.org/10.5194/hess-16-4603-2012
Li D, Long D, Zhao J, Lu H, Hong Y (2017) Observed changes in flow regimes in the Mekong River Basin. J Hydrol 551:217–232. https://doi.org/10.1016/j.jhydrol.2017.05.061
Liu KT, Tseng KH, Shum CK, Liu CY, Kuo CY, Liu G, Jia Y, Shang K (2016) Assessment of the impact of reservoirs in the Upper Mekong River using satellite radar altimetry and remote sensing imageries. Remote Sens 8(5):367. https://doi.org/10.3390/RS8050367
Ly S, Try S, Sayama T (2021) Hydrological changes in the Mekong River Basin under future hydropower developments and reservoir operations. J Japan Soc Civ Eng Ser (hydrol Eng) 77(2):259–264. https://doi.org/10.2208/jscejhe.77.2_I_259
Mann HB (1945) Non-parametric test against trend. Econometrica 13:245–259. https://doi.org/10.2307/1907187
Massey FJ (1951) The Kolmogorov-Smirnov test for goodness of fit. J Am Stat Assoc 46:68–78. https://doi.org/10.1080/01621459.1951.10500769
MRC (2005) Overview of the hydrology of the Mekong Basin. Mekong River Commission, Vientiane
MRC (2009) Database of the existing, under construction and planning/proposed hydropower projects in the Lower Mekong Basin. Mekong River Commission, Vientiane
MRC (2011) Assessment of basin-wide development scenarios—main report. Mekong River Commission, Vientiane
MRC (2019a) The MRC hydropower mitigation guidelines, vol 1. Mekong River Commission, Vientiane
MRC (2019b) Snapshot of the MRC council study* findings and recommendations. Mekong River Commission, Vientiane
Nash JE, Sutcliffe JV (1970) River flow forecasting through conceptual models part I—a discussion of principles. J Hydrol 10(3):282–290. https://doi.org/10.1016/0022-1694(70)90255-6
Ngo LA, Masih I, Jiang Y, Douven W (2018) Impact of reservoir operation and climate change on the hydrological regime of the Sesan and Srepok Rivers in the Lower Mekong Basin. Clim Change 149(1):107–119. https://doi.org/10.1007/S10584-016-1875-Y

Perera EDP, Sayama T, Magome J, Hasegawa A, Iwami Y (2017) RCP8.5-based future flood hazard analysis for the Lower Mekong River Basin. Hydrology 4(4):55. https://doi.org/10.3390/HYDROLOGY4040055
Pettitt AN (1979) A non-parametric approach to the change-point problem. Appl Stat 28(2):126. https://doi.org/10.2307/2346729
Piman T, Cochrane TA, Arias ME (2016) Effect of proposed large dams on water flows and hydropower production in the Sekong, Sesan and Srepok Rivers of the Mekong Basin. River Res Appl 32(10):2095–2108. https://doi.org/10.1002/rra.3045
Piman T, Cochrane TA, Arias ME, Green A, Dat DN (2013a) Assessment of flow changes from hydropower development and operations in Sekong, Sesan, and Srepok Rivers of the Mekong Basin. J Water Resour Plan Manag 139(6):723–732. https://doi.org/10.1061/(ASCE)WR.1943-5452.0000286
Piman T, Lennaerts T, Southalack P (2013b) Assessment of hydrological changes in the Lower Mekong Basin from basin-wide development scenarios. Hydrol Process 27(15):2115–2125. https://doi.org/10.1002/hyp.9764
Pokhrel Y, Shin S, Lin Z, Yamazaki D, Qi J (2018) Potential disruption of flood dynamics in the Lower Mekong River Basin due to upstream flow regulation. Sci Rep 8(1):17767. https://doi.org/10.1038/s41598-018-35823-4
Räsänen TA, Koponen J, Lauri H, Kummu M (2012) Downstream hydrological impacts of hydropower development in the Upper Mekong Basin. Water Resour Manag 26(12):3495–3513. https://doi.org/10.1007/s11269-012-0087-0
Räsänen TA, Someth P, Lauri H, Koponen J, Sarkkula J, Kummu M (2017) Observed river discharge changes due to hydropower operations in the Upper Mekong Basin. J Hydrol 545:28–41. https://doi.org/10.1016/j.jhydrol.2016.12.023
Sayama T, Ozawa G, Kawakami T, Nabesaka S, Fukami K (2012) Rainfall–runoff–inundation analysis of the 2010 Pakistan flood in the Kabul River Basin. Hydrol Sci J 57(2):298–312. https://doi.org/10.1080/02626667.2011.644245
Sayama T, Tatebe Y, Iwami Y, Tanaka S (2015) Hydrologic sensitivity of flood runoff and inundation: 2011 Thailand floods in the Chao Phraya River Basin. Nat Hazards Earth Syst Sci 15(7):1617–1630. https://doi.org/10.5194/NHESS-15-1617-2015
Sen PK (1968) Estimates of the regression coefficient based on Kendall's Tau. J Am Stat Assoc 63(324):1379–1389. https://doi.org/10.1080/01621459.1968.10480934
Shin S, Pokhrel Y, Yamazaki D, Huang X, Torbick N, Qi J, Pattanakiat S, Ngo-Duc T, Nguyen TD (2020) High resolution modeling of river-floodplain-reservoir inundation dynamics in the Mekong River Basin. Water Resour Res 56(5):e2019WR026449. https://doi.org/10.1029/2019WR026449
Singh J, Knapp HV, Arnold JG, Demissie M (2005) Hydrological modeling of the Iroquois River watershed using HSPF and SWAT. JAWRA J Am Water Resour Assoc 41(2):343–360. https://doi.org/10.1111/J.1752-1688.2005.TB03740.X
Sridhar V, Kang H, Ali SA (2019) Human-induced alterations to land use and climate and their responses for hydrology and water management in the Mekong River Basin. Water 11(6):1307. https://doi.org/10.3390/w11061307
Try S, Lee G, Yu W, Oeurng C, Jang C (2018) Large-scale flood-inundation modeling in the Mekong River Basin. J Hydrol Eng 23(7):05018011. https://doi.org/10.1061/(ASCE)HE.1943-5584.0001664
Try S, Tanaka S, Tanaka K, Sayama T, Hu M, Sok T, Oeurng C (2020a) Projection of extreme flood inundation in the Mekong River Basin under 4k increasing scenario using large ensemble climate data. Hydrol Process 34(22):4350–4364. https://doi.org/10.1002/hyp.13859
Try S, Tanaka S, Tanaka K, Sayama T, Khujanazarov T, Oeurng C (2022a) Comparison of CMIP5 and CMIP6 GCM performance for flood projections in the Mekong River Basin. J Hydrol Reg Stud 40:101035. https://doi.org/10.1016/J.EJRH.2022.101035
Try S, Tanaka S, Tanaka K, Sayama T, Lee G, Oeurng C (2020b) Assessing the effects of climate change on flood inundation in the Lower Mekong Basin using high-resolution AGCM outputs. Prog Earth Planet Sci 7(1):1–16. https://doi.org/10.1186/s40645-020-00353-z
Try S, Tanaka S, Tanaka K, Sayama T, Oeurng C, Uk S, Takara K, Hu M, Han D (2020c) Comparison of gridded precipitation datasets for rainfall-runoff and inundation modeling in the Mekong River Basin. PLoS ONE 15(1):e0226814. https://doi.org/10.1371/journal.pone.0226814
Varis O, Kummu M, Salmivaara A (2012) Ten major rivers in monsoon asia-pacific: an assessment of vulnerability. Appl Geogr 32(2):441–454. https://doi.org/10.1016/J.APGEOG.2011.05.003
Vörösmarty CJ, Sharma KP, Fekete BM, Copeland AH, Holden J, Marble J (1997) The storage and aging of continental runoff in large reservoir systems of the world. Ambio 26(4):210–219
Wang W, Lu H, Ruby Leung L, Li HY, Zhao J, Tian F, Yang K, Sothea K (2017) Dam construction in Lancang-Mekong River Basin could mitigate future flood risk from warming-induced intensified rainfall. Geophys Res Lett 44(20):10378–10386. https://doi.org/10.1002/2017GL075037
Wild TB, Loucks DP (2014) Managing flow, sediment, and hydropower regimes in the Sre Pok, Se San, and Se Kong Rivers of the Mekong Basin. Water Resour Res 50(6):5141–5157. https://doi.org/10.1002/2014WR015457
Wright S (1921) Correlation and causation. J Agric Res 20:557–585
Yamazaki D, Ikeshima D, Tawatari R, Yamaguchi T, O'Loughlin F, Neal JC, Sampson CC, Kanae S, Bates PD (2017) A high-accuracy map of global terrain elevations. Geophys Res Lett 44(11):5844–5853. https://doi.org/10.1002/2017GL072874
Yun X, Tang Q, Wang J, Liu X, Zhang Y, Lu H, Wang Y, Zhang L, Chen D (2020) Impacts of climate change and reservoir operation on streamflow and flood characteristics in the Lancang-Mekong River Basin. J Hydrol 590:125472. https://doi.org/10.1016/J.JHYDROL.2020.125472
Zhong R, Zhao T, Chen X (2021) Evaluating the tradeoff between hydropower benefit and ecological interest under climate change: how will the water-energy-ecosystem nexus evolve in the Upper Mekong Basin. Energy 237:121518. https://doi.org/10.1016/J.ENERGY.2021.121518
Ziese M, Rauthe-Schöch A, Becker A, Finger P, Meyer-Christoffer A, Schneider U (2018) GPCC full data daily version.2018 at 1.0°: daily land-surface precipitation from rain-gauges built on gts-based and historic data. Global Precipitation Climatology Centre

Publisher's Note